A Small Deletion Hotspot in the Type II Keratin Gene *mK6irs1/Krt2-6g* on Mouse Chromosome 15, a Candidate for Causing the Wavy Hair of the Caracul (*Ca*) Mutation

Yoshiaki Kikkawa,*,[1] Ayumi Oyama,*,†,[1] Rie Ishii,*,[1] Ikuo Miura,* Takashi Amano,† Yoshiyuki Ishii,‡ Yasuhiro Yoshikawa,‡ Hiroshi Masuya,§ Shigeharu Wakana,§ Toshihiko Shiroishi,§ Choji Taya* and Hiromichi Yonekawa*,[2]

**Department of Laboratory Animal Science, The Tokyo Metropolitan Institute of Medical Science (Rinshoken), Tokyo 113-8613, Japan, †Department of Zootechnical Science, Tokyo University of Agriculture, Atsgi, Kanagawa 243-0034, Japan, ‡Department of Biomedical Science, The University of Tokyo, Tokyo 113-8657, Japan and §Mouse Functional Genomics Research Group, RIKEN Genome Science Center, The Institute of Physical and Chemical Research, Yokohama 244-0804, Japan*

Manuscript received January 30, 2003
Accepted for publication June 4, 2003

ABSTRACT

A new mutation has arisen in a colony of mice transgenic for human α-galactosidase. The mutation is independent of the transgenic insertion, autosomal dominant, and morphologically very similar to the classical wavy coat mutation, caracul (*Ca*), on chromosome 15. Therefore, we designated this locus the caracul Rinshoken (Ca^{Rin}). Applying a positional cloning approach, we identified the *mK6irs1/Krt2-6g* gene as a strong candidate for Ca^{Rin} because among five *Ca* alleles examined mutations always occurred in the highly conserved positions of the α-helical rod domain (1A and 2B subdomain) of this putative gene product. The most striking finding is that four independently discovered alleles, the three preexistent alleles Ca^{J}, Ca^{9J}, Ca^{10J}, and our allele Ca^{Rin}, all share one identical amino acid deletion (N 140 del) and the fifth, Ca^{medJ}, has an amino acid substitution (A 431 D). These findings indicate that a mutation hotspot exists in the *Ca* locus. Additionally, we describe a *Ca* mutant allele induced by ENU mutagenesis, which also possesses an amino acid substitution (L 424 W) in the *mK6irs1/Krt2-6g* gene. The identification of the *Ca* candidate gene enables us to further define the nature of the genetic pathway required for hair formation and provides an important new candidate that may be implicated in human hair and skin diseases.

THE keratins constitute a group of >40 highly insoluble proteins that serve as the subunits forming intermediate filament polymers in epithelial cells (O'Guin *et al.* 1990; Fuchs 1995). In addition to the epithelial or soft α-keratins, this multigene family also contains a smaller subfamily of hard α-keratins, which, because of their most common site of occurrence, are generally referred to as hair keratins. Previous protein studies indicated that, independent of the species, the hair keratin family consists of four individual members per subfamily, which were designated hair acidic, type-I keratin (*Krt1*) and hair basic, type II keratin (*Krt2*), respectively (Heid *et al.* 1986; Lynch *et al.* 1986). Keratins are expressed as obligate heterodimers of *Krt1/Krt2* pairs in a tissue- and differentiation-specific fashion.

Keratin gene products play an important role in the mechanical support of hair development. Such a role has been confirmed in the context of transgenic mouse models (Powell and Rogers 1990; Magin 1998) and through mutations in several keratin genes that have been found to cause a variety of diseases affecting hair development in humans (Irvine and McLean 1999). Over the past several years, hair keratin research has made considerable progress. Thus, the entire sets of human type I and type II hair keratin genes, as well as the patterns of expression of the encoded proteins, have been elucidated (Rogers *et al.* 1998, 2000; Langbein *et al.* 1999, 2001). In particular, the hair follicle has been found to contain both hair keratins and epithelial keratins. The former are found in the hair fiber and the latter in the inner and outer root sheath. One of the epithelial keratins, mK6IRS1/KRT2-6G, the product of the *mK6irs1/Krt2-6g* gene, is expressed exclusively in the inner root sheath and could therefore play an important role in hair development and/or hair morphology through its influence on hair follicle cell development, although this simplified scheme can elucidate in part either the processes or the mechanisms on the development.

Sequence data from this article have been deposited with the DDBJ/EMBL/GenBank Data Libraries under accession nos. AB100413–AB100418.

[1]These authors contributed equally to this work.

[2]*Corresponding author:* Department of Laboratory Animal Science, The Tokyo Metropolitan Institute of Medical Science (Rinshoken), 3-18-22, Honkomagome Bunkyo-ku, Tokyo 113-8613, Japan. E-mail: yonekawa@rinshoken.or.jp

Regarding the development of hair follicle cells, in the early stage the epithelium arose from the ectoderm, a single layer of pluripotent cells that can differentiate to either follicle or epidermis. The critical process depends upon whether the ectoderm can contact a condensate of specialized mesenchyme called the dermal papillae. A mesenchymal signal triggers an ectodermal cell to proliferate and the cells grow downward to form a hair germ. An ectodermal signal leads these epithelial cells in the dermal papillae to differentiate further and to develop into a hair follicle, forming a compartment of stem cells, a sebaceous gland, and a hair shaft surrounded by an outer and inner root sheath. Although the wingless/integrated and Sonic hedgehog (SHH) signaling pathway clearly participate in the developmental processes of both follicle and epidermis, less is known about the former (Hardy 1992; Fuchs 2001; Miller 2002).

The periods of hair growth are followed by a regression phase (the catagen phase), when the lower part of the follicle undergoes programmed cell death, and a resting phase (the telogen phase), before onset of a new growth phase (the anagen phase). Cyclical growth of hair continues throughout postnatal life, allows the follicle to remodel itself, and occurs randomly in humans but in a synchronized manner in mice (Miller 2002).

Mouse hair keratin genes colocalize with epithelial keratin genes on the distal portion of chromosome 11 (*Krt1*) and the distal portion of chromosome 15 (*Krt2*). In both of these regions there are several previously described mutations that cause abnormal hair: on chromosome 11, the mutations rex (*Re*), recombination-induced mutation 3 (*Rim3*), and whiskers amiss (*wam*) and on chromosome 15, caracul (*Ca*), shaven (*Sha*), velvet coat (*Ve*), naked (*N*), and Hague (*Hag*) (Dunn 1937; Doolittle *et al.* 1996; Sato *et al.* 1998; Taylor *et al.* 2000; Poirier *et al.* 2002).

While constructing human α-galactosidase transgenic mice (Kase *et al.* 1988), we isolated a mutant with an abnormal coat hair phenotype. The new mutant is a single autosomal dominant, and the phenotype has a strong resemblance to that caused by the *Ca* mutation (Dunn 1937). The locus was also mapped distal to chromosome 15, which is very close to the *Ca* locus; therefore, we named the new mutation caracul Rinshoken (Ca^{Rin}). Using positional cloning, we discovered that a deletion of one amino acid residue, aspartic acid, had occurred in the *mK6irs1/Krt2-6g* coding sequence, which is therefore a candidate for the *Ca* mutation. Next, we searched for mutations in five *Ca* alleles, each of which had been independently discovered in the Jackson Laboratory (JAX alleles), and sought *N*-ethyl-*N*-nitrosourea (ENU)-induced wavy coat hair mutants isolated during the RIKEN mutagenesis project. This study resulted in the identification of mutations in the *mK6irs1/Krt2-6g* coding sequence of four JAX alleles and one ENU-induced allele. Interestingly, three other alleles possess a deletion identical to that found in Ca^{Rin}, suggesting that a germline mutation hotspot does exist in the *Ca* locus.

MATERIALS AND METHODS

Mice: The Ca^{Rin} mutant arose spontaneously in a C57BL/6slc (B6) mouse during the production of human α-galactosidase cDNA transgenics. This founder mouse was fixed as a mutant strain and bred in the animal facility at The Tokyo Metropolitan Institute of Medical Science (Rinshoken). Heterozygous Ca^{Rin} mice were crossed to MSM/Ms (MSM) or JF1/Ms (JF1) strain animals to generate intersubspecific backcross progeny for linkage analysis. The MSM and JF1 are inbred strains established from the Japanese wild mouse (Moriwaki 1994; Kikkawa *et al.* 2001) and maintained at the National Institute of Genetics. Five mutants with other *Ca* alleles, B6C3Fe-a/a-Ca^{medJ}, BALB/cBy-Ca^{10J}, BALB/cBy-Ca^{9J}, C3HeB/FeJ-$Ca^{J/+Hm/+Sl/+}$, and C57BL/6By-Ca^{Sl}, and their background strains were purchased from the Jackson Laboratory (JAX) as genomic DNA samples. Two ENU-induced mutant lines, M100573 and M100689, were provided from RIKEN Genome Science Center (GSC). For mutagenesis, ENU was administered to C57BL/6J male mice (G_0). Sequence analyses were performed using G_2 animals with the genetic background of DBA/2J × (DBA/2J × ENU-treated C57BL/6J)F_1. The detailed protocol of ENU mutagenesis is described on the RIKEN GSC website (http://www.gsc.riken.go.jp/Mouse/).

Linkage analysis: A total of 321 backcross progeny were typed for the wavy coat hair of the *Ca* phenotype and then genomic DNA was prepared from liver and/or pinna skin and used for linkage analysis. Microsatellite markers were purchased from Research Genetics/Invitrogen (San Diego). Simple sequence length polymorphisms (PCR-SSLP) were analyzed: 1 μl (100 ng) of genomic DNA was amplified in a total volume of 15 μl with final concentrations of 1× Gold buffer II, 1.5 mM $MgCl_2$, 200 μM dNTPs, 0.25 μM of each primer, and 0.1 units AmpliTaq Gold polymerase (Applied Biosystems, Foster City, CA). Reactions were carried out in the GeneAmp 9700 thermal cycler with a PCR profile of one cycle at 95° for 5 min and 40 cycles of 94° for 30 sec, 55° for 40 sec, and 72° for 60 sec. PCR products were loaded on 4% agarose gels (3% NuServe agarose and 1% agarose). PCR primers for eight *Krt2* genes were designed according to the published mRNA sequences (Table 1). These primer pairs amplified a fragment corresponding to the 5′- and 3′-untranslated region (UTR). The chromosomal location of these genes was determined by linkage analysis through key recombinants by single-strand conformation polymorphism (PCR-SSCP). Linkage analysis was performed with the Map Manager QXP (Manly *et al.* 2001).

Bacterial artificial chromosome analysis: A mouse CITB bacterial artificial chromosome (BAC) library was screened at Research Genetics/Invitrogen by PCR with 3′-end markers of *Krt2* genes. DNA from positive clones was isolated by the alkaline lysis method (Sambrook *et al.* 1989) and then analyzed by pulsed field gel electrophoresis. BAC ends were directly sequenced with T7 and SP6 primers. To determine if their BAC-end-derived sequences mapped to mouse chromosome 15, PCR primers for these ends were synthesized (Table 1) and then used to map these PCR products through key recombinants by PCR-SSCP. Details of these BAC-end-derived primer sequences are given in Table 1.

Mutation screening: To screen for mutations between B6 and Ca^{Rin}, total RNA was isolated from 5-week-old mouse skin by using TRIzol (Life Technologies/Invitrogen) following the manufacturer's protocol. cDNA was generated with the Omniscript RT kit (QIAGEN, Valencia, CA) using 1 μg of DNase-

TABLE 1

STS primers developed in this study

Source	Primer sequence		Product size (bp)
	Forward 5′–3′	Reverse 5′–3′	
Krt2 gene[a]			
Krt2-1-5′	AGAGGAGTTCTCAGCTCCTTCCATCTC	GCTGACTAGGCCAGCAGAGCCTGAG	146
Krt2-1-3′	ACCAAATAAAGAGGTGACCACCG	TTACCATGGGACTCAGACTGC	209
Krt2-4-5′	CTTCTGTTCTAAGCTCGTTGCAGCTGC	GCCGCCGCCTTGGCAGGACCCAGCCAC	260
Krt2-4-3′	ATAGGCGAGACGGGATCCTGAT	AGTTGAGAAGAAGCTACCAGGTTCC	207
Krt2-5-5′	GCCGCGTAGACAACATCCAGCTCAC	GTGCGCTGATGCAGCAGCGGTTGCC	137
Krt2-5-3′	TAGTGACAGGTCCTCCAAATGAGC	ATCTGAAGACAGGTTGGGGTTAAGG	230
Krt2-6a-5′	GCTCAACACACTCATCTCTTCAGCTC	CTGAGCTGGCACTGTAGCCACGGTGG	133
Krt2-6a-3′	GCTACAGGCAGTGAATTCTGTCACC	GTGAATTGTGATGTAAGCTCACAGG	230
Krt2-6b-5′	CCATATATAAGCCACAGTCCAGAGCTC	CACTCTGGCTGAGCTGGCACTGTAG	169
Krt2-6b-3′	TCTTCTGGTGGCCTCAGCTCTTCCACC	TCTGGGGTCTGCAACAAGCTCTGGTAG	113
K6irs-5′	CTTCCTCCTGCACCTTTACTCCATCC	CTCCTGCCACCTCCCAGGCTGTAGAG	199
K6irs-3′	GCCTCCGTCCTCACCACACTACCTG	GTCTTCTTCTTGGGTACAGCTCTAG	120
Krt2-7-3′	TGGGAAGCAATGCTCTGAGCTTCAG	AGCAGTTTCAGACTATCTTCCAGGC	186
Krt2-8-5′	CGAACCTCCGTCTTCAGCTCACTG	CCACTCGTGAACGAGCGGCTGCTG	127
Krt2-8-3′	AAGTGAATGGCCACTGAAGTCCTTG	AAGCCATTGGGATATCCCAGATAGG	172
Krt2-10-3′	AAGTGGCCTGGACTACAAGGCTAAG	TATTCCCAGGGCTGCAGCTGAGGCA	168
Krt2-16-5′	CTGAAGGCTCTCTACCATGAGGAAATCGAG	GCACACTGAGCCTTGGTATGCTCG	294
Krt2-16-3′	ACCAGGTACTGAGCACCTAG	ACTGCTTTCGGTAGTAGTGC	238
Krt2-17-5′	GGAATATTCACTCGTCTTGCTGAGC	CCAGAGACCACAGCTGAACCGCTACTG	132
Krt2-17-3′	AGGTGTGACCTTCTCCTTTAG	AACGGCTTGAAGACACACTTGG	237
Krt2-19-3′	CTGGCTTCTAGAAGTCCCTTTGGAG	TGTGGCTCTCTAGCTACTGGCTCAC	107
BAC end			
310F1-T7	TGCTGAGGCCGGAAGATGAAGTAAG	AAGCAGACCTCCTTCATCCTTCAGC	211
310F1-SP6	CACTCTGGCCTTAATACTTGGCAG C	TTTCTCTATGTTGCCCTGGCTGACG	115
298P5-T7	AGCGTCTCAGGTCCTGTGACCTGAG	AGAAGTCATCTCTCCTTGAGCTTGC	124
298P5-SP6	CTCCTGTCTGAGTCAAGATCTACTG	TTAGCCCAGCAGGAAGTGACATTGG	150
363H8-T7	CTTTTAAGCCCTCCCTGTTGCATTC	CTCCTACTGTCAAGCATTCTGATAC	171
363H8-SP6	GCCAACAGGTGGCACACAATATTCT	CTCTTCCAATCTTACGGAATCACC	91
304H2-T7	GATCTTCTTGGGATTGAGTACATATC	GACTGTCCCAGGTGCGGAACTACTG	198
304H2-SP6	TCCACTGAGAACTCATAGAACTGCC	ATGTGTAGATGTGCTTGTGTGTATAGG	204
51L7-T7	AGTCCTCAAGAACTTACGCC	GCAGATGATACCTAGAGAGAGG	147
51L7-SP6	AAGTTCTAGAAAGGTATGATACATG	TGTGGTTCAGATCAAGTCAAGGCTG	99

[a] These primer pairs amplified a fragment corresponding to the 5′ and 3′ noncoding region.

pretreated total RNA. The entire genomic region of the *mK6irs1/Krt2-6g* gene was amplified to give overlapping PCR products from five mutant mice with other *Ca* alleles; two ENU-induced mutant lines, M100573 and M100689; and their background strains (C57BL/6Jslc, C57BL/6J, BALB/cBy, C3HeB/FeJ, and DBA/2J) by long and accurate (LA) PCR (Takara, Otsu, Japan) using the primers corresponding to each exon: exons 1–7, *K6irs*5′F and R5; exons 6 and 7, *K6irs*F5 and R14; exons 7–9, *K6irs*F7 and R9. Sequences of these primers are shown in Table 2. PCR products were gel purified, sequenced using BigDye Terminator cycle sequencing kits, and analyzed on a 3100 genetic analyzer (Applied Biosystems).

RT-PCR and Northern blot hybridization: Approximately 1 μg of DNase-pretreated total RNA prepared from cDNA obtained from B6 and B6-*Ca*^{Rin} skin (5 weeks old) was reverse transcribed using the Omniscript RT kit. The cDNA was amplified for 30 cycles (94° for 30 sec, 60° for 30 sec, 72° for 1 min) using AmpliTaq Gold and a 9700 Thermocycler (Applied Biosystems). The products were subjected to agarose gel electrophoresis. Primers used for detection of *K6irs/Krt2-6g*-specific transcripts were *K6irs*F7 and *K6irs*R4. This product was a 755-bp stretch derived from the 3′ coding sequence and part of the 3′-UTR.

Total RNA (20 μg per lane) was loaded onto a 1% agarose-formaldehyde gel and transferred onto Hybond N+ membrane (Amersham, Arlington Heights, IL). The filter was hybridized with a randomly labeled (Amersham) probe in Rapid-hyb buffer (Amersham) at 70° for 12 hr and then washed (2× SSC, 0.1% SDS) at room temperature for 20 min, followed by stringent washing (0.1× SSC, 0.1% SDS) at 65° for 15 min. The *K6irs/Krt2-6g* probe was the above-mentioned 755-bp fragment. Blots were stripped and hybridized with a mouse *Gapdh* probe.

Histological analysis: Dorsal skin was dissected from B6 and B6-*Ca*^{Rin} at 5 weeks of age and fixed in 4% paraformaldehyde overnight. After fixation, the tissues were dehydrated, embedded in paraffin, sectioned (6 μm), and stained with hematoxylin and eosin.

We carried out immunohistofluorescence analysis using polyclonal antibody against *mK6IRS1/KRT2-6G*, at a dilution of 1:3200. The antibody against *mK6IRS1/KRT2-6G* was kindly provided by Y. Shimomura and M. Ito (Department of Derma-

TABLE 2

PCR and sequencing primers for *mK6irs1/Krt2-6g* gene developed in this study

Primer name	Primer sequence: 5′–3′	Primer position	
		cDNA	Genomic
*K6irs*5′F	CTTCCTCCTGCACCTTTACTCCATCC	17–42	1–26
*K6irs*R6	TGAGACAAGAGCTGTTCCCAGG	—	503–524
*K6irs*F11	GACTGGTGGATCATGAAC	—	871–888
*K6irs*R11	TGATGCTGTCTCCTCCAC	—	2136–2153
*K6irs*F3	TTCTTGGAGCAGCAGAACCAGGTGCTG	502–508	2624–2650
*K6irs*R3	ACCACGTCACGCACATTCCTCAG	670–692	2792–2814
*K6irs*F12	ACCCTTCCTCTTTGACTC	—	3330–3347
*K6irs*F4	TATGAGGAGGAGATCAACCGGCGG	712–735	3759–3782
*K6irs*R13	CTTGTGAGTAACATGCAAG	—	4435–4453
*K6irs*F13	CTCTCTATTCCAAGGCCTC	—	4460–4478
*K6irs*F5	CCAGGAGCTGCAGCTGGCAGCTGG	1035–1058	5013–5036
*K6irs*R5	TTCTCAATCTCTGAGCGGAGTCTCTGG	1119–1145	5097–5123
*K6irs*R15	GTCTCTAGGTTAGAAGC	1159–1175	6315–6331
*K6irs*F7	GCTTCTAACCTAGAGACAGCCATCG	1159–1183	6315–6339
*K6irs*R14	TTAGGCTCATGAGCTCCTGATATTCACGC	1290–1318	6446–6474
*K6irs*F17	TTCTTTACCAGCACAGGTAC	—	6932–6951
*K6irs*F18	CAGTGGCTTGGAAGATGC	—	7554–7571
*K6irs*R4	GAGGAAGCCCAGATGGAGACCCAAG	1890–1914	8849–8873
*K6irs*R9	CAGGGAGGGCTTAAAAGAATACAAG	2121–2145	9075–9099

tology, Niigata Graduate School of Medicine & Dental Science, Niigata, Japan; Aoki *et al.* 2001). For immunofluorescence, FITC-coupled rabbit IgG (Molecular Probes, Eugene, OR) was used at a dilution of 1:1000.

RESULTS

Description of phenotype: During transgenesis experiments with human α-galactosidase cDNA (Kase *et al.*

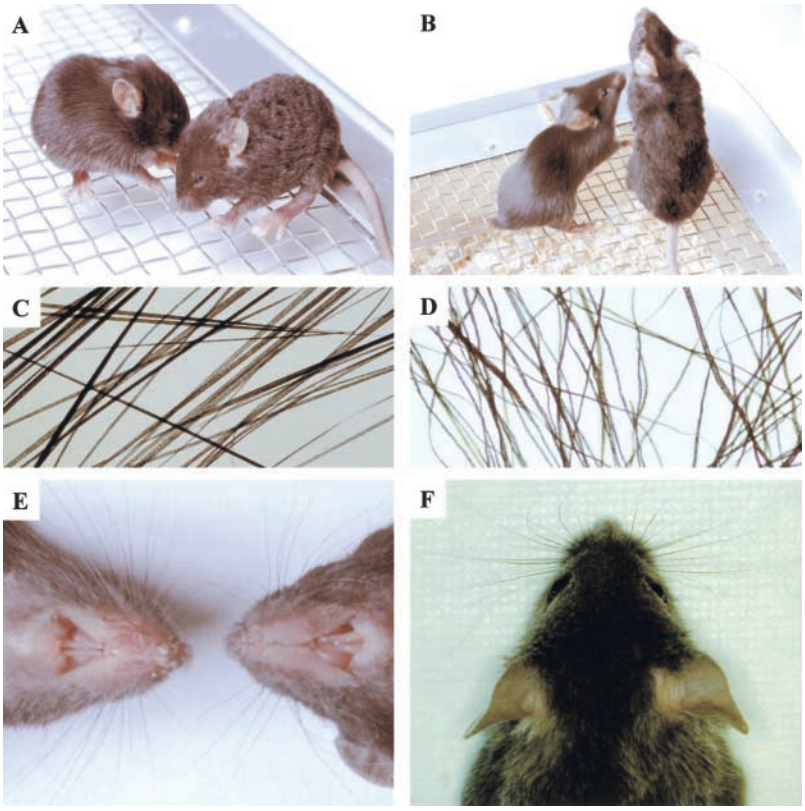

Figure 1.—Phenotype of hair coat and whiskers. (A) Hair coat at 3 weeks of age in normal (left) and C57BL/6slc-Ca^{Rin} (right). Wavy hair coat can be seen in this mutant. (B) Hair coat at 12 weeks of age in normal (left) and C57BL/6slc-Ca^{Rin}/− (right). After 4 weeks, the wavy coat hair phenotype is less apparent, but the hair looks plush like. (C and D) Comparison of hair texture phenotype between normal (C) and Ca^{Rin} mouse (D) at 12 weeks. Note the disordered hairs, as at 12 weeks, with irregular curls and kinks in hair of the whole body. (E) Ventral view of head (whiskers) of C57BL/6slc mice comparing normal (left) and Ca^{Rin} (right). (F) Whiskers and hair coat at 8 weeks of age in an ENU-induced mutant, M100689.

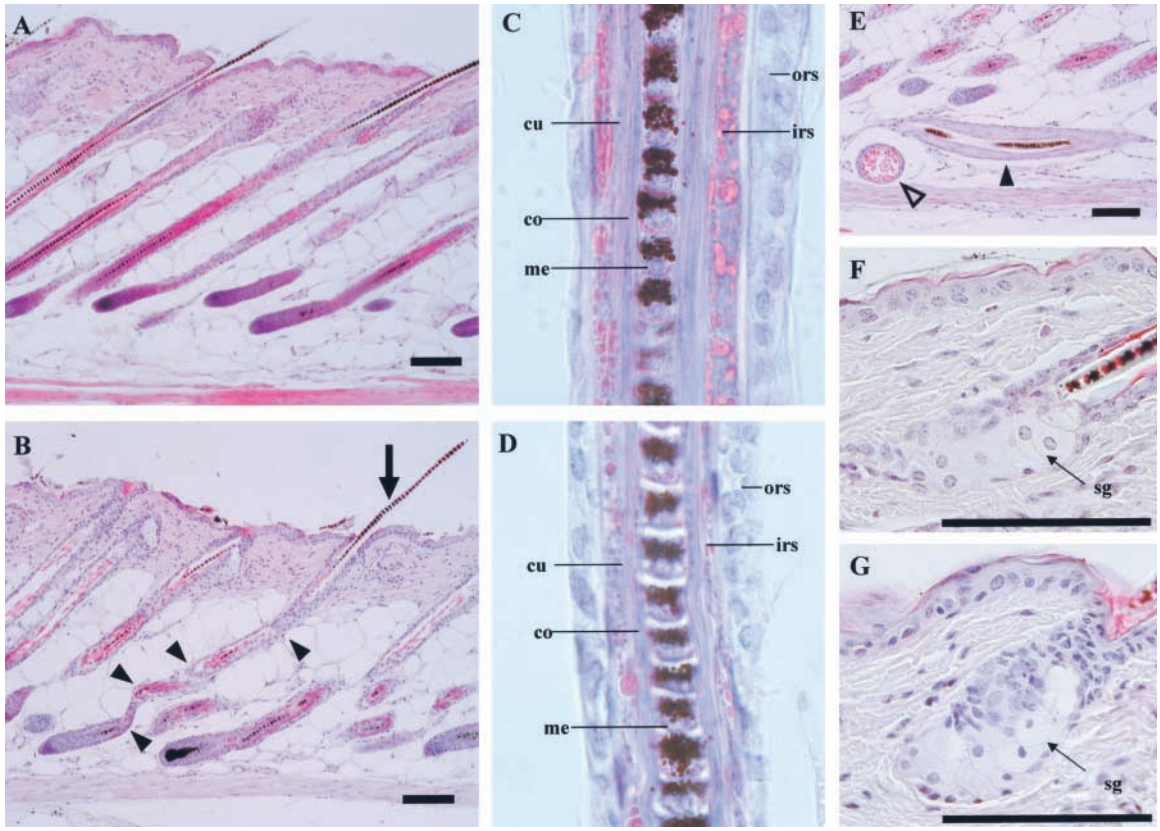

FIGURE 2.—Dorsal skin sections from control (A) and Ca^{Rin} (B) mice at 5 weeks. Normal anagen hair follicles (A) have straight hairs with a tightly compacted IRS structure (C), whereas the follicles of the mutant are twisted and/or curved (B). A follicle in B is twisted at least four times (arrowheads) producing waved hair (arrow). Severely curved follicles in E have grown alongside the subcutaneous layer. One of them is sectioned longitudinally (E, solid arrowhead), and the other is cut transversely (E, open arrowhead). Comparison of sebaceous glands (sg) of control (F) and Ca^{Rin} (G) mice at 5 weeks. A hair follicle-derived cyst is observed in the dermis. Sebaceous glands are enlarged around the cyst structure (arrows). Hematoxylin and eosin staining; ors, outer root sheath; irs, inner root sheath; cu, cuticle; co, cortex; me, medulla. Bar, 100 μm.

1988), we isolated a mutant mouse carrying an abnormal coat hair phenotype. Southern blot analysis of affected individuals revealed that their genome did not contain any human genetic components, suggesting that the mutation occurred independently in the transgenic mouse colony. Animals carrying the new mutant are easily distinguished from their nonaffected littermates, because of the following phenotype: (1) the mutant mice exhibit rough and greasy fur and (2) their hair is wavy and pointed in different directions (Figure 1A), with the wavy appearance prominent between 3 and 6 weeks of age. Thus, there is a strong resemblance to individuals carrying the *Ca* mutation (DUNN 1937). In the affected progeny, whiskers are markedly curved, and coat hair is wavy from the time of first appearance until postweaning age (~4 weeks), as is also the case in the original *Ca* mutant (Figure 1, A and E). After 4 weeks, the waviness of the coat hair became much less apparent, and the hair acquired a plush-like morphology (Figure 1, B–D). An ENU-induced mutant, M100689, also shows a similar phenotype of hair coat and whiskers (Figure 1F).

All of the F_1 progeny showed the mutant phenotype using at least 100 progeny in reciprocal crosses (data not shown), with the heterozygotes being phenotypically indistinguishable from the homozygotes. We are thus dealing with a single autosomal dominant mutation. The mutated locus was mapped distal to chromosome 15, very close to the *Ca* locus, and thus we named the new mutation caracul Rinshoken (Ca^{Rin}).

Histological observation revealed that the dorsal skin of 5-week-old mutant mice was thinner than that of age-matched controls, mainly because of decreased thickness of the adipose layer (Figure 2, A and B). At this age, the dorsal skin hair follicles were at the second anagen stage in both the mutant and control mice. In contrast to hair follicles of nonaffected littermates, the follicles of mutants were curved and twisted randomly, thus producing wavy hair (Figure 2B). The extent of curvature was different in each follicle. In severe cases, curved follicles had grown alongside the subcutaneous muscle layer (Figure 2, E and F). Moreover, the mutant follicles exhibited abnormal morphology of the inner root sheath (IRS): namely, the IRS lacked uniformity of thickness and, in some follicles, the IRS cells showed abnormal

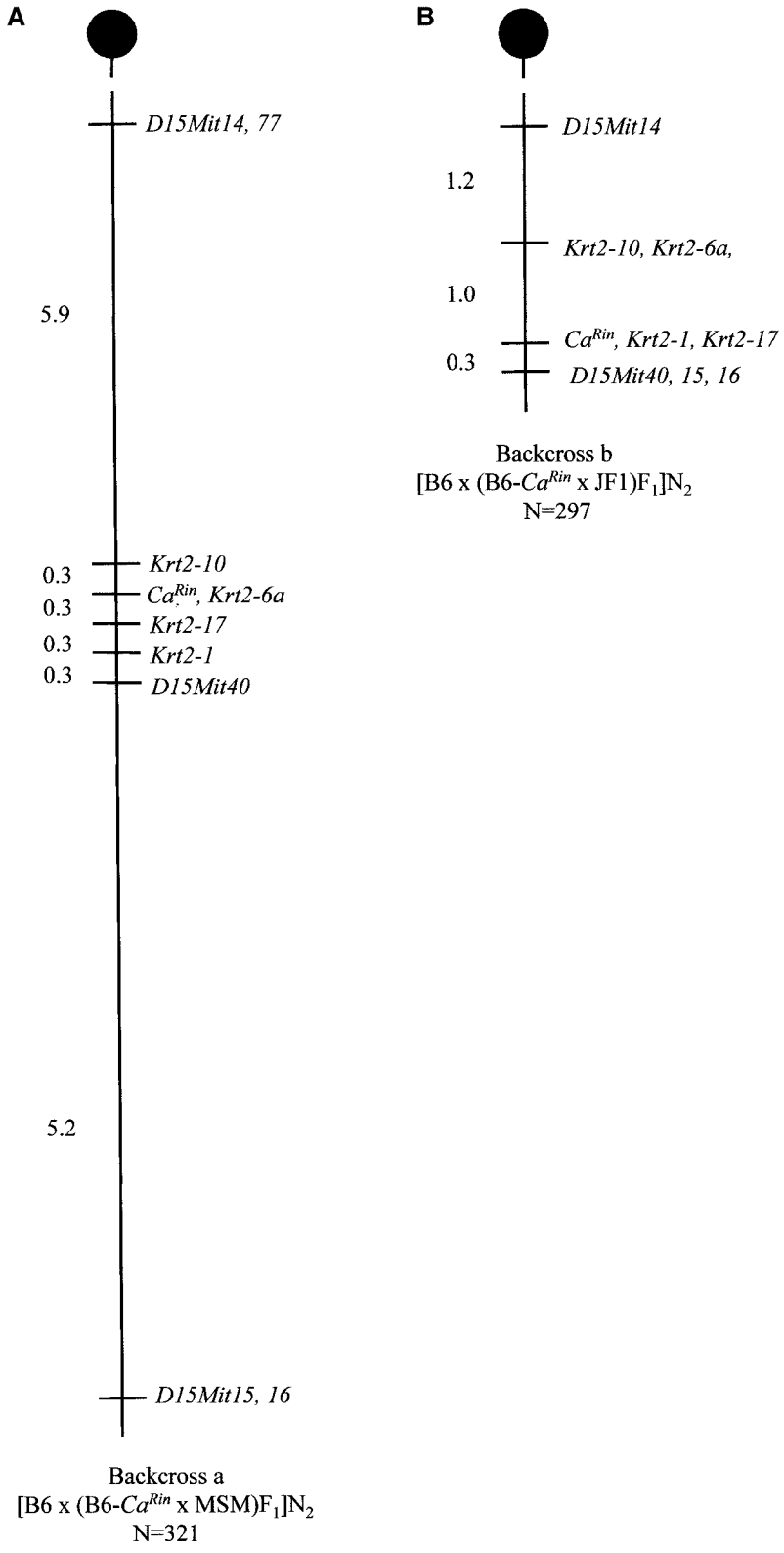

FIGURE 3.—Linkage map of the region around the Ca^{Rin} locus on mouse chromosome 15. (A) Markers shown were typed in 321 progeny from the MSM cross: C57BL/6J × (C57BL/6J-Ca^{Rin}/Ca^{Rin} × MSM/Ms)F_1. (B) Markers shown were typed in 297 progeny from the JF1 cross: C57BL/6J × (C57BL/6J-Ca^{Rin}/Ca^{Rin} × JF1/Ms)F_1. Map distances between adjacent loci are shown in centimorgans on the left.

keratinization (Figure 2, C and D). In addition to these abnormalities, follicular-derived cysts containing keratin debris were occasionally observed in the dermis. The mutant mouse sebaceous glands were larger than those of control mice and this was particularly marked around the cyst structures (Figure 2G).

Linkage mapping of Ca^{Rin}: In small scale intersubspecific backcrossing between B6-Ca^{Rin}/Ca^{Rin} and MSM/Ms (backcross a), we first determined that the Ca^{Rin} locus mapped to the distal region of chromosome 15 (data not shown). We then extended the number of backcross segregants to 321 and subjected all to *Ca* phenotyping.

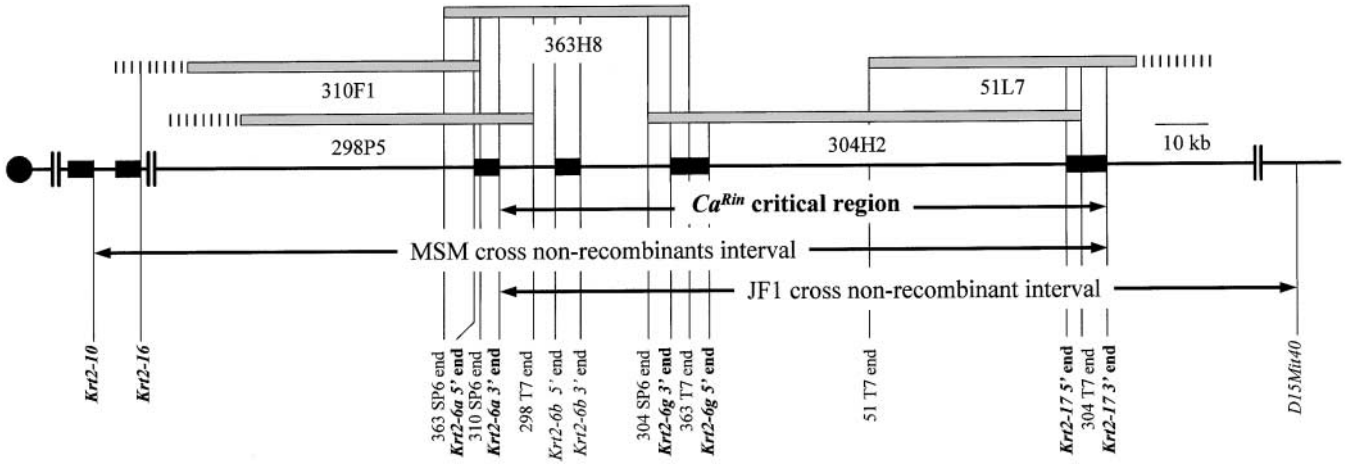

FIGURE 4.—BAC-based physical map. Chromosome 15 is indicated as a horizontal line with the chromosome centromere designated by a solid circle. *Krt2* genes are shown as solid boxes overlying the horizontal line. BAC clones are positioned as shaded boxes over the horizontal line and drawn to scale. The marker content of each clone is designated by vertical lines connecting the clone with chromosome 15. The nonrecombinant intervals defined by linkage analysis using two-intersubspecific backcross are also shown. The critical interval is indicated by an arrow.

They were also genotyped by molecular markers flanking the Ca^{Rin} locus: *D15Mit14* and *D15Mi77* [*D15Mit14/77*] as a proximal marker and *D15Mit40* as a distal marker (Figure 3A). There were 19 recombination events between *D15Mit14/77* and Ca^{Rin} and 4 between Ca^{Rin} and *D15Mit40*. The Ca^{Rin} locus was therefore located within this 7.5-cM interval. We also generated other intersubspecific backcrosses between B6-Ca^{Rin}/

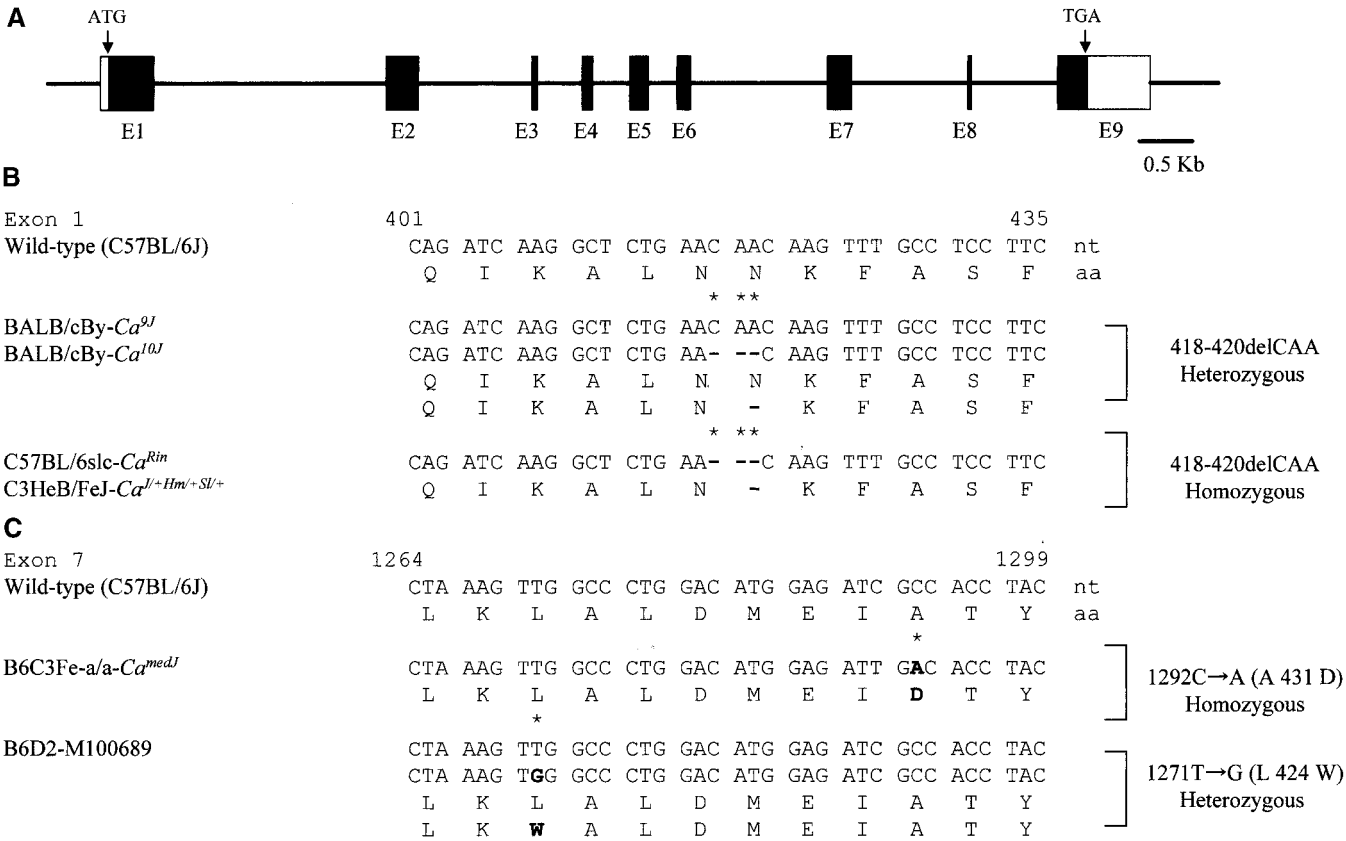

FIGURE 5.—*mK6irs1/Krt2-6g* gene mutations in five *Ca* alleles and the ENU-induced wavy coat mutant, M100689. (A) A schematic illustration of the genomic structure of the mouse *mK6irs1/Krt2-6g* gene depicts the translation initiation codon, exon numbers, and a stop codon. (B and C) Sequence analysis of exon 1 (B) and exon 7 (C) in wild type, *Ca* alleles, and M100689. Asterisks mark the mutation positions. (B) Heterozygous and homozygous 418-AAC-420 deletion found in Ca^{Rin}, Ca^{J}, Ca^{9J}, and Ca^{10J}. (C) Heterozygous 1271T → G (L424W) missense substitution and homozygous 1292C to A (A431D) missense substitutions found in M100689 and Ca^{medJ}, respectively.

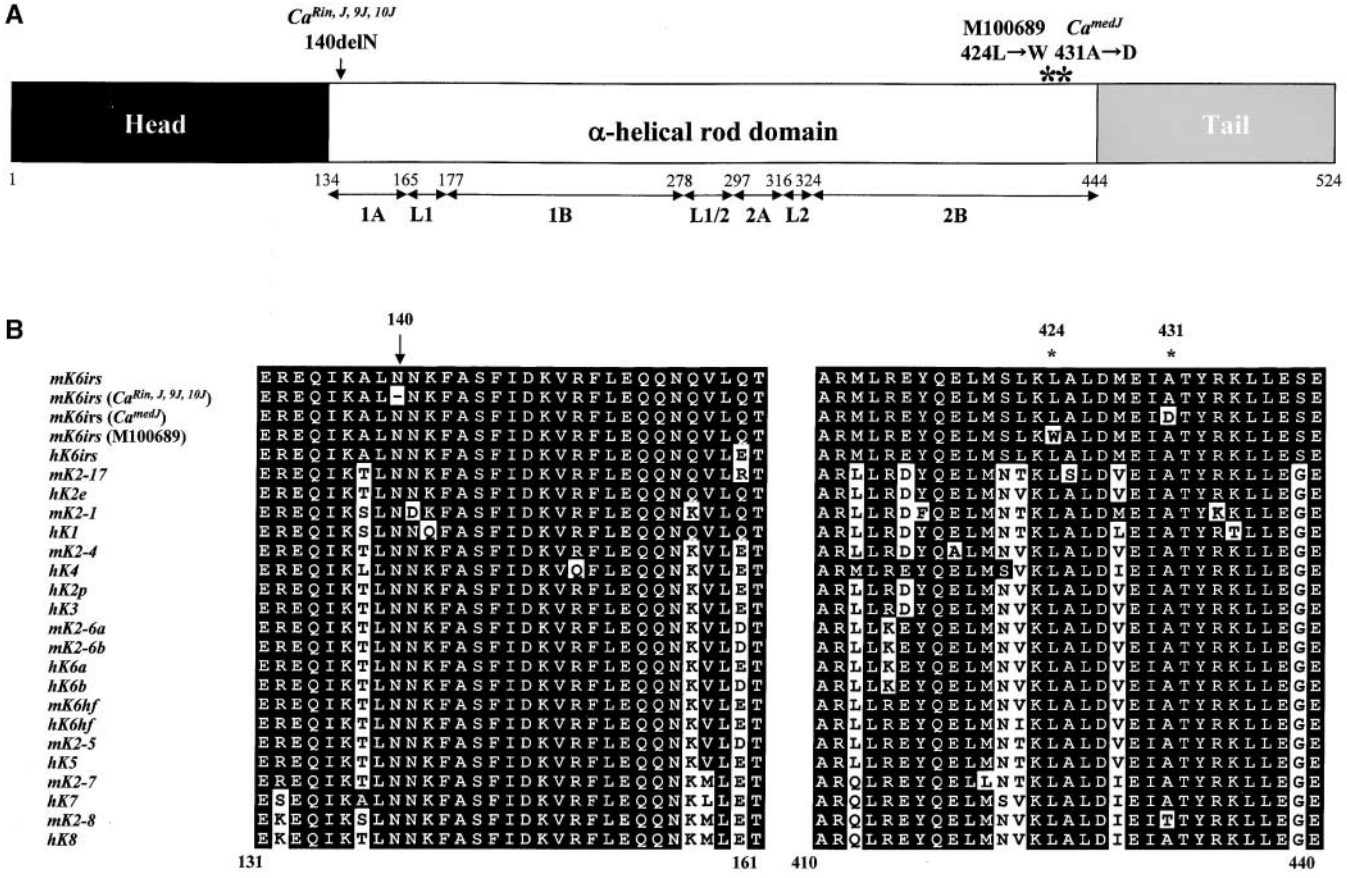

FIGURE 6.—*mK6irs1/Krt2-6g* is mutated in *Ca* mice. (A) Amino acid sequence of the *mK6irs1/Krt2-6g* gene. The central α-helical rod domain is shown as an open box, the subdomains of which are marked by double-headed arrows. The amino acid deletion in Ca^{Rin}, Ca^{J}, Ca^{9J}, and Ca^{10J} is indicated by an arrow, and the point mutation in Ca^{medJ} and the ENU-induced wavy coat mutant, M100689, is marked with an asterisk. (B) Alignment of protein sequence in the human and mouse type II epithelial keratins. Arrow (deletion in Ca^{Rin}, Ca^{J}, Ca^{9J}, and Ca^{10J}) and asterisks (point mutation in Ca^{medJ} and M100689) mark the mutation positions. Both mutations occur in the highly conserved sequence of the α-helical rod domain of this protein. The amino acid sequences of the α-helical rod domain used for multiple alignments of the type II epithelial keratins of mouse (m) and human (h) were derived from the following cDNA sequence of the GenBank/EMBL database: *mK6irs/Krt2-6g* (AOKI *et al.* 2001, accession no. NM_019956); *hK6irs/Krt2-6g* (LANGBEIN *et al.* 2001, NM_033448); *mK2-17* (HERZOG *et al.* 1994, X74784); hK2e (COLLIN *et al.* 1992a, AF019084); *mK2-1* (STEINERT *et al.* 1985, NM_008473); *hK1* (STEINERT *et al.* 1985, NM_006121); *mK2-4* (KNAPP *et al.* 1986, NM_008475); *hK4* (LEUBE *et al.* 1988, NM_002272); *hK2p* (COLLIN *et al.* 1992b, Q01546); *hK3* (MOLL *et al.* 1982, NM_057088); *mK2-6a* (TAKAHASHI *et al.* 1998, NM_008476); *mK2-6b* (TAKAHASHI *et al.* 1998, NM_010669); *hK6a* (TAKAHASHI *et al.* 1995, NM_005554); *hK6b* (TAKAHASHI *et al.* 1995, NM_005555); *mK6hf* (POIRIER *et al.* 2002, AF343088); *hK6hf* (WINTER *et al.* 1998, NM_004693); *mK2-5* (CARNINCI and HAYASHIZAKI 1999, NM_027011); *hK5* (LERSCH and FUCHS 1988, NM_000424); *mK2-7* (CARNINCI and HAYASHIZAKI 1999, NM_033073); *hK7* (GLASS and FUCHS 1988, NM_005556); *mK2-8* (VASSEUR *et al.* 1985, NM_031170); and *hK8* (LEUBE *et al.* 1986, NM_002273). Multiple sequence alignment was performed using the CLUSTAL W program.

Ca^{Rin} and JF1 (backcross b) and examined 297 segregants. Linkage analysis was done with the same molecular markers as above. The order of the markers was identical to that of backcross a, but there was a striking difference regarding the genetic distances between the adjacent markers. Thus, the distance between *D15Mit14/77* and Ca^{Rin} is 6.2 cM in backcross a, whereas it is only 2.2 cM in backcross b. Similarly, the Ca^{Rin} and *D15Mit15/16* interval is 5.8 cM in backcross a, whereas it is only 0.3 cM in backcross b (Figure 3).

Because the 12 *Krt2* loci, *Krt2-1*, *-4*, *-6a*, *-6b*, *-6g*, *-7*, *-8*, *-10*, *-16*, *-17*, *-18*, and *-19*, had all been previously mapped to the Ca^{Rin} region of mouse chromosome 15 (Mouse Genome Informatics: http://www.informatics.jax.org/), we tried to superimpose these *Krt2* loci on our maps. For this purpose, we used the sequence-tagged site (STS) markers derived from the 5′- and 3′-UTR sequences of these *Krt2* genes to genotype the loci using PCR-SSCP analysis. Four STS markers from the *Krt2* genes mentioned above, *Krt2-1* (5′), *Krt2-6a* (3′), *Krt2-10* (3′), and *Krt2-17* (5′), mapped to the region critical for the Ca^{Rin} locus, because the polymorphisms were found in each *Krt2*-STS marker between B6 and MSM. Linkage showed that the *Krt2-10* locus mapped proximal to Ca^{Rin} with one recombination event; the *Krt2-17* locus mapped distal to Ca^{Rin} with one recombi-

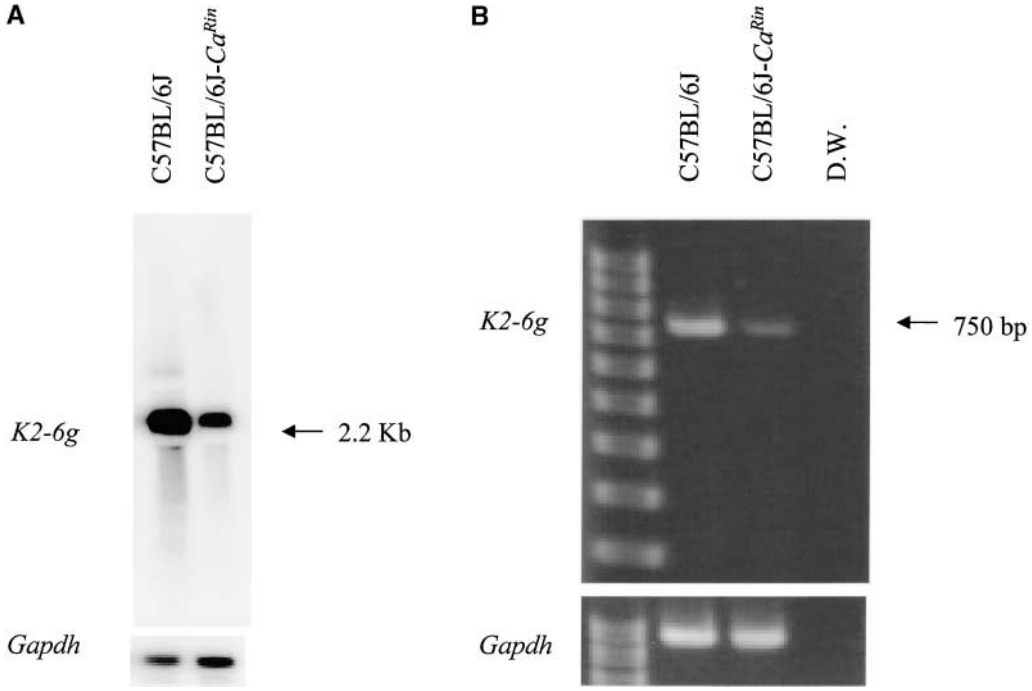

FIGURE 7.—Northern blot (A) and RT-PCR (B) analyses of *K6irs/Krt2-6g*. Total RNA was obtained from 5-week-old skin. (A) *K6irs/Krt2-6g* expression levels were reduced in Ca^{Rin}. The primary *K6irs/Krt2-6g* RNA is ~2.2 kb. The blot was subsequently rehybridized with *Gapdh*. (B) To detect *K6irs/Krt2-6g*-specific transcripts, cDNA from B6 and B6-Ca^{Rin} skin was screened with the primers *K6irs7F* and *K6irs4R* located in different exons. cDNA was amplified as a 750-bp *K6irs/Krt2-6g* product (top arrow; Table 2). The 1-kb *Gapdh* control band is also indicated (bottom).

nation event; and the *Krt2-6a* mapped at the same position as Ca^{Rin} in the backcross a progeny (Figure 3A). On the other hand, linkage showed that *Krt2-10/6a* mapped proximal to Ca^{Rin} with three recombination events and that *Krt2-1/17* mapped to the same position as Ca^{Rin} in the backcross b progeny (Figure 3B). The Ca^{Rin} locus, therefore, was located between *Krt2-6a* and *Krt2-17*.

Physical mapping of the Ca^{Rin} locus: To construct a physical map of the Ca^{Rin} region, the linkage map was used as a scaffold to assemble a BAC contig. The core of the physical map was *Krt2-6a* and *Krt2-17*, the markers closest to Ca^{Rin}. Five overlapping BACs (310F1, 298P5, 363H8, 304H2, and 51L7) were isolated from BAC libraries using the STS markers derived from these two *Krt2* genes and BAC-end sequences (Figure 4). Further characterization of this BAC contig by PCR-based approaches using STS markers derived from the 5′- and 3′-UTR sequences of the *Krt2* gene confirmed that this contig contained the *Krt2-6b* and *mK6irs1/Krt2-6g* genes as well as *Krt2-6a* and *Krt2-17*. This physical map indicated that the gene order of *Krt2* is proximal: *Krt2-6a*, *Krt2-6b*, *mK6irs1/Krt2-6g*, *Krt2-17* (Figure 4). Thus, we narrowed down the Ca^{Rin} nonrecombinant interval and concluded that it contains only four *Krt2* genes, namely, *Krt2-6a*, *Krt2-6b*, *mK6irs1/Krt2-6g*, and *Krt2-17*, which are therefore strong candidates for Ca^{Rin}.

***mK6irs1/Krt2-6g* mutations in *Ca*:** To evaluate these four positional candidates, *Krt2-6a*, *Krt2-6b*, *mK6irs1/Krt2-6g*, and *Krt2-17*, we carried out RT-PCR analysis to compare the sequences of Ca^{Rin} and +/+ (B6) skin cDNA. We did not find any mutations in the coding regions of *Krt2-6a*, *Krt2-6b*, and *Krt2-17* (data not shown). However, in the sequence of the *mK6irs1/Krt2-6g* gene, we identified a 3-bp deletion (CAA) at nucleotide positions 418–420, causing an asparagine deletion at amino acid position 140, which lies in the α-helical rod domain (Figures 5 and 6). Asparagine 140 is highly conserved among other epithelial keratin genes in mouse and human, compared to other members including this gene family (Figure 6B).

To identify mutations in the other *Ca* alleles, Ca^{J}, Ca^{medJ}, Ca^{9J}, Ca^{10J}, and Ca^{Sl}, we undertook genomic sequencing of the *mK6irs1/Krt2-6g* gene using DNA purchased from the Jackson Laboratory. Using a combination of long-range PCR with direct sequencing, we determined the nucleotide sequence of a 9.3-kb genomic DNA containing all exons and introns of the *mK6irs1/Krt2-6g* gene (GenBank accession nos. AB100414–AB100418). Nucleotide sequence comparison revealed the three nucleotide deletions in exon 1 of Ca^{J}, Ca^{9J}, and Ca^{10J} to be completely identical to the deletion found in Ca^{Rin} (Figure 5). A different *mK6irs1/Krt2-6g* mutation was identified in Ca^{medJ}, a C to A conversion at exon 7 predicted to substitute aspartic acid for alanine at position 431 (Figures 5 and 6A). At the same position of the murine *Krt2-8* gene, an A to T amino acid substitution was discovered (Figure 6B). To date, we do not know whether the substitution is a mutation causing a phenotype change. Further studies, such as transgenesis of genomic clones derived from the Ca^{medJ} mutant, will clarify this issue. On the last allele, Ca^{Sl}, we could not detect any mutations in the *mK6irs1/Krt2-6g* gene with this technique.

Further, we have carried out the same analysis in two ENU-induced wavy hair mutants. One point mutation was identified in one mutant, M100689, a T to G trans-

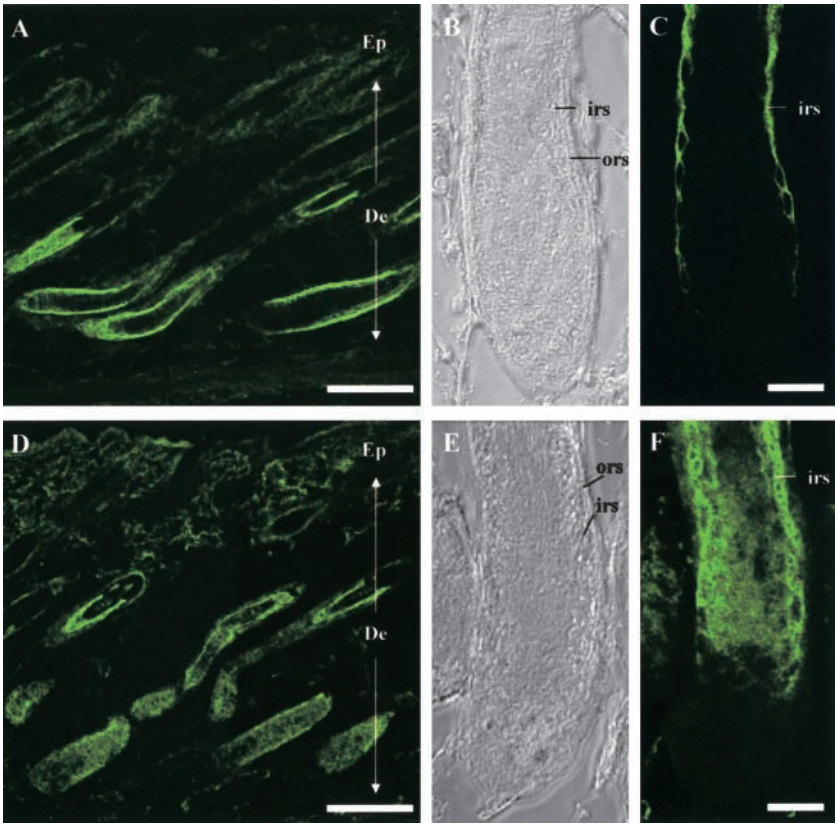

FIGURE 8.—Immunohistochemical comparison using anti-K6IRS/KRT2-6G polyclonal antibody between wild-type and mutant Ca^{Rin} mice. Tissue distribution of K6IRS/KRT2-6G protein in the wild-type (A and C) and Ca^{Rin} (D and F) mouse hair follicles at 5 weeks is shown. Using the *K6irs/Krt2-6g* polyclonal antibody, K6IRS/KRT2-6G protein is detected with a distinct distribution in the IRS of hair follicles in the wild-type mouse (A and C), whereas it has a rather fuzzy distribution in the mutant Ca^{Rin} mice (D and F). Phase-contrast microscopy in the same area of wild-type (B) and mutant mice (E) is also shown. Ep, epidermis; De, dermis; irs and ors, inner and outer root sheath, respectively. Bar in A and D, 100 μm; in C and F, 20 μm.

version in exon 7 predicted to result in the substitution of tryptophan for leucine at amino acid position 424 (Figures 5 and 6A). This leucine at 424 is also highly conserved among other epithelial keratin genes in mouse and human (Figure 6B). In another mutant, M100573, we could not detect any mutations in the *mK6irs1/Krt2-6g* gene with this approach.

To examine the effect of the Ca^{Rin} mutation on *mK6irs1/Krt2-6g* RNA expression, we carried out Northern blot and RT-PCR analysis using RNA isolated from the skin of 5-week-old +/+ and Ca^{Rin}/Ca^{Rin} mice. We selected this source because AOKI *et al.* (2001) had reported that of the major murine tissues, *mK6irs1/Krt2-6g* expression was found only in skin and was highest at the anagen stage. The level of *mK6irs1/Krt2-6g* expression was markedly reduced in Ca^{Rin} by both Northern blot and RT-PCR analysis (Figure 7).

AOKI *et al.* (2001) reported that *mK6irs1/Krt2-6g* is expressed in the Huxley and Henle layers of mouse inner hair sheath. To examine whether the expression pattern of *mK6irs1/Krt2-6g* is also retained in the Ca^{Rin} mutant mice, we compared the localization of the mK6IRS1/KRT2-6G protein in the hair follicle between the mutant and wild-type mice (Figure 8). As AOKI *et al.* (2001) reported, the mK6IRS1/KRT2-6G protein was expressed exclusively in the inner root sheath (Figure 8, A–C) in wild-type mice. On the other hand, the specificity of the mK6IRS1/KRT2-6G protein did evidently decrease in the Ca^{Rin} mutant mice (Figure 8, D–F). For example, the inner root sheath of the mutant mice was most strongly stained but the majority of the hair shaft was also weakly stained. This suggests that dysregulated mK6IRS1/KRT2-6G protein localization occurred in the mutant mice.

DISCUSSION

A type II keratin gene, *mK6irs1/Krt2-6g*, as the candidate for *Ca* mutation: Using a positional cloning approach, we discovered that a strong candidate for the gene affected by the caracul (*Ca*) mutation is a type II keratin gene, *mK6irs1/Krt2-6g*, because five independent *Ca* alleles exhibit mutations in the *mK6irs1/Krt2-6g* gene (Figure 5). The Ca^{Rin} allele contains a small in-frame 3-bp deletion at nucleotides 420–422 in the first exon of the *mK6irs1/Krt2-6g* gene and this deletion putatively causes a one-amino-acid (asparagine) deletion. This asparagine deletion is located in a highly conserved region in the 310-amino-acid coiled-coil rod domain (α-helical domain; Figure 6A). The α-helical domain functions to form heteropolymers consisting of a specific type I and a type II cytokeratin through interactions of these domains (HATZFELD and WEBER 1990). VASSAR *et al.* (1991) showed that transgenic mice expressing a deleterious allele of human K14 displayed dominant-negative inhibition of endogenous cytokeratin expression mediated via the mutated α-helical domain functions, *i.e.*; these mice exhibited abnormalities

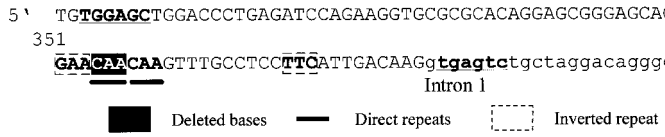

FIGURE 9.—A hotspot of small deletions in the mouse *K6irs/Krt2-6g* gene. The region surrounding position 420 of the coding region in exon 1 is represented. One proposed mechanism of the deletion would be slippage of DNA polymerase through these repeat sequences. Inverted repeats are another mechanism that causes loops on a single DNA strand and they were indeed present, flanking the deletion in this case. Sequence motifs in the vicinity of position 420 that may account for the small deletion hotspot are represented. The small deletion consensus sequences are underlined.

in epidermal architecture and often died prematurely. Therefore, the pathobiology and biochemistry of the transgenic mice and their cultured keratinocytes bore resemblance to a group of genetic disorders known as epidermolysis bullosa simplex. As another example of associated pathology, transgenic mice carrying a dominant-negative *Krt2-6a* gene suffered severe blistering and neonatal death (WOJCIK *et al.* 1999). Because the Ca^{Rin} phenotype is dominant and deleterious for hair texture and IRS morphology (Figures 1 and 2), it is very likely that the asparagine deletion causes an alteration in the mK6IRS1 coiled-coil domain and a resultant dominant-negative phenotype. Furthermore, the expression of mK6IRS1 mRNA is markedly decreased in the skin of Ca^{Rin} mice, even in the anagen phase, when *mK6irs1/Krt2-6g* message peaked in nonaffected littermates (Figure 7). Assuming that the level of *mK6irs1/Krt2-6g* transcription is proportional to translation, this finding suggests that stoichiometric lack of the mK6IRS1 protein occurs in the cells and subsequently causes the decreased availability of heteropolymers. The same is true for the Ca^{medJ} allele, where a single C to A transversion generated an amino acid substitution of an aspartic acid for an alanine at position 431, which is highly conserved within the α-rod helical domain; *i.e.*, all type II keratin genes examined contain an alanine residue at this position (Figure 6). The ENU-induced *Ca* allele can also be explained in the same way. It is suggested that this amino acid replacement destroys the tertiary structure of the molecule and consequently prevents protein-protein interactions between the other cytokeratin counterparts.

A small deletion hotspot in *mK6irs1/Krt2-6g* gene: We examined five *Ca* mutations and found that four of these, the preexistent alleles Ca^{J}, Ca^{9J}, Ca^{10J}, and our allele Ca^{Rin}, shared the same small deletion (Figures 5 and 6). Because these alleles were independently derived (see JAX catalog; http://www.jax.org/jaxmice), this suggests that a mutation hotspot causing a small deletion is present in the first exon of the *mK6irs1/Krt2-6g* gene. If so, this is the first description that such a hotspot is present in the mouse. In humans, such hotspots have been reported in the *SMAD4* gene in juvenile polyposis patients (HOWE *et al.* 2002) and in the interferon gamma receptor 1 (*IFNGR1*) gene associated with dominant susceptibility to mycobacterial infection (JOUANGUY *et al.* 1999). To date, little is known about precise molecular mechanisms responsible for hotspots. However, two main mechanisms causing such deletions have been proposed, namely slippage of DNA polymerase and slipped mispairing (JOUANGUY *et al.* 1999; HOWE *et al.* 2002). Both events are thought to be caused by the interactions between specific DNA sequences such as direct repeats, inverted repeats, palindromes, or a small deletion consensus motif and enzymes for DNA replication (GRUNDY *et al.* 1991; KRAWCZAK and COOPER 1991, 1993). In this murine small deletion hotspot, we found two direct repeats of CAA at nucleotides 417–419 and 420–422, either of which is deleted in the mutations, in the first exon of the *mK6irs1/Krt2-6g* gene. Two consensus motifs TG (A/G) (A/G) (G/T) (A/C) or (A/G) also exist in the first exon and intron 1 (Figure 9). Taking this evidence together with the lack of an intervening and polypurine sequence (JOUANGUY *et al.* 1999), it is likely that slippage of DNA polymerase occurs in the *mK6irs1/Krt2-6g* gene.

Role of *mK6irs1/Krt2-6g* in hair formation: To date, the mK6IRS1/KRT2-6G molecule is the protein that is expressed exclusively in the IRS, in particular, in the Henle and Huxley layers of the hair follicle in IRS (AOKI *et al.* 2001; PORTER *et al.* 2001; LANGBEIN *et al.* 2002), although previous reports claimed the expression of other type I and II cytokeratins in IRS, such as K1, K10, K13, and K16 (STARK *et al.* 1990). Furthermore, its expression is stage specific in the hair cell cycle, *i.e.*, can be detected during the hair follicle growth phase, but hardly at all at any other stage (AOKI *et al.* 2001). We confirmed the restricted expression of the mK6IRS1/KRT2-6G protein in IRS and furthermore we discovered that the expression pattern is disturbed in the Ca^{Rin} mutant mice (Figure 8). These lines of evidence suggest that the mK6IRS1/KRT2-6G protein plays important roles in the development of hair and the maintenance of the cells in the IRS (AOKI *et al.* 2001; PORTER *et al.* 2001; LANGBEIN *et al.* 2002). The findings documented here that the *mK6irs1/Krt2-6g* gene is a strong candidate for that causing the *Ca* mutation shed new light on its possible function(s), because phenotype analyses of the *Ca* mutant indicate that it causes abnormal hair texture as well as abnormal morphology in the IRS (Figures 1 and 2). Because the IRS surrounds the hardening hair fiber and the central hair-forming unit proper, the *Ca* mutation is considered as causing primarily a defect in IRS function. In particular, the evidence that the IRS of *Ca* mice lacked uniformity of thickness and in some follicles the IRS cells showed abnormal keratinization (Figure 2) supports this contention. These lines of evidence suggest that the IRS

most likely functions as a "corset" or a "barrel" molding the hair into its optimal shape during its progression toward the skin surface. Consequently, defects in the IRS compromise the correct shaping of the hair fiber, thus creating a wavy type.

It has been reported that the cytokeratin genes are involved in several spontaneous skin diseases in humans (Vassar *et al.* 1991; Chapalain *et al.* 2002). To date, no such spontaneous diseases associated with cytokeratin mutations have been reported in mice. On the other hand, mice with manipulated cytokeratin genes do show abnormalities; *e.g.*, animals expressing a deleterious allele of the human K14 gene in the basal epidermis developed a cutaneous phenotype bearing some resemblance to the human disorder epidermolysis bullosa simplex (Vassar *et al.* 1991), and mice carrying a mutated *Krt2-6a* transgene suffered severe blistering and neonatal death (Wojcik *et al.* 1999). These lines of evidence suggest that we may be able to generate a useful model for human skin diseases through the manipulation of cytokeratin genes in mice and, in addition, facilitate the understanding of the function(s) of the gene in the IRS. We are now trying to generate such gene-manipulated mice using the *mK6irs1/Krt2-6g* gene.

We thank Satomi Yamada and Yayoi Wakita of The Tokyo Metropolitan Institute of Medical Science and Kimio Kobayashi, Aya Shimizu, and Junko Nagano of Riken GSC for technical assistance. We are also grateful to Yutaka Shimomura and Masaaki Ito of Niigata University of School of Medicine for giving us the anti-mK6IRS1/KRT2-6G polyclonal antibody and to Kiyokazu Morioka of The Tokyo Metropolitan Institute of Medical Science for valuable comments on hair morphology and development. This research was supported by a Grant-in-Aid for Scientific Research (13680919) from the Japanese Society for the Promotion of Science and by a Health Sciences Research Grant (Research on Eye and Ear Science, Immunology, Allergy, and Organ Transplantation) from the Ministry of Health, Labor, and Welfare of Japan.

LITERATURE CITED

Aoki, N., S. Sawada, M. A. Rogers, J. Schweizer, Y. Shimomura *et al.*, 2001 A novel type II cytokeratin, mK6irs, is expressed in the Huxley and Henle layers of the mouse inner root sheath. J. Invest. Dermatol. **116:** 359–365.

Carninci, P., and Y. Hayashizaki, 1999 High-efficiency full-length cDNA cloning. Methods Enzymol. **303:** 19–44.

Chapalain, V., H. Winter, L. Langbein, J. M. Le Roy, C. Labreze *et al.*, 2002 Is the loose anagen hair syndrome a keratin disorder? A clinical and molecular study. Arch. Dermatol. **138:** 501–506.

Collin, C., R. Moll, S. Kubicka, J. P. Ouhayoun and W. W. Franke, 1992a Characterization of human cytokeratin 2, an epidermal cytoskeletal protein synthesized late during differentiation. Exp. Cell Res. **202:** 132–141.

Collin, C., J. P. Ouhayoun, C. Grund and W. W. Franke, 1992b Suprabasal marker proteins distinguishing keratinizing squamous epithelia: cytokeratin 2 polypeptides of oral masticatory epithelium and epidermis are different. Differentiation **51:** 137–148.

Doolittle, D. P., M. T. Davisson, J. N. Guidi and M. C. Green, 1996 Catalog of mutant genes and polymorphic loci, pp. 17–854 in *Genetic Variants and Strains of the Laboratory Mouse*, Ed. 3, edited by M. F. Lyon, S. Rastan and S. D. M. Brown. Oxford University Press, Oxford.

Dunn, L. C., 1937 Caracul, a dominant mutation. J. Hered. **28:** 334.

Fuchs, E., 1995 Keratins and the skin. Annu. Rev. Cell. Dev. Biol. **11:** 123–153.

Fuchs, E., 2001 *The Harvey Lectures*, Series 94, pp. 47–78. Wiley-Liss, New York.

Glass, C., and E. Fuchs, 1988 Isolation, sequence, and differential expression of a human K7 gene in simple epithelial cells. J. Cell Biol. **107:** 1337–1350.

Grundy, C. B., F. Thomas, D. S. Millar, M. Krawczak, E. Melissari *et al.*, 1991 Recurrent deletion in the human antithrombin III gene. Blood **78:** 1027–1032.

Hardy, M. H., 1992 The secret life of the hair follicle. Trends Genet. **8:** 55–61.

Hatzfeld, M., and K. Weber, 1990 The coiled coil of in vitro assembled keratin filament is a heterodimer of type I and II keratins: use of site-specific mutagenesis and recombinant protein expression. J. Cell Biol. **110:** 1199–1210.

Heid, H. W., E. Werner and W. W. Franke, 1986 The complement of native alpha-keratin polypeptides of hair-forming cells: a subset of eight polypeptides that differ from epithelial cytokeratins. Differentiation **32:** 101–119.

Herzog, F., H. Winter and J. Schweizer, 1994 The large type II 70-kDa keratin of mouse epidermis is the ortholog of human keratin K2e. J. Invest. Dermatol. **102:** 165–170.

Howe, J. R., J. Shellnut, B. Wagner, J. C. Ringold, M. G. Sayed *et al.*, 2002 Common deletion of SMAD4 in juvenile polyposis is a mutational hotspot. Am. J. Hum. Genet. **70:** 1357–1362.

Irvine, A. D., and W. H. McLean, 1999 Human keratin diseases: the increasing spectrum of disease and subtlety of the phenotype-genotype correlation. Br. J. Dermatol. **140:** 815–828.

Jouanguy, E., S. Lamhamedi-Cherradi, D. Lammas, S. E. Dorman, M. C. Fondaneche *et al.*, 1999 A human IFNGR1 small deletion hotspot associated with dominant susceptibility to mycobacterial infection. Nat. Genet. **4:** 370–378.

Kase, R., M. Shimmoto, K. Itoh, K. Utsumi, M. Kotani *et al.*, 1988 Immunohistochemical characterization of transgenic mice highly expressing human lysosomal alpha-galactosidase. Biochim. Biophys. Acta **1406:** 260–266.

Kikkawa, Y., I. Miura, S. Takahama, S. Wakana, Y. Yamazaki *et al.*, 2001 Microsatellite database for MSM/Ms and JF1/Ms, molossinus-derived inbred strains. Mamm. Genome **12:** 750–752.

Knapp, B., M. Rentrop, J. Schweizer and H. Winter, 1986 Nonepidermal members of the keratin multigene family: cDNA sequences and in situ localization of the mRNAs. Nucleic Acids Res. **14:** 751–763.

Krawczak, M., and D. N. Cooper, 1991 Gene deletions causing human genetic disease: mechanisms of mutagenesis and the role of the local DNA sequence environment. Hum. Genet. **86:** 425–441.

Krawczak, M., and D. N. Cooper, 1993 Gene deletion, pp. 163–208 in *Human Gene Mutations*, edited by M. Krawczak and D. N. Cooper. Bios Scientific Publishers, Oxford.

Langbein, L., M. A. Rogers, H. Winter, S. Praetzel, U. Beckhaus *et al.*, 1999 The catalog of human hair keratins. I. Expression of the nine type I members in the hair follicle. J. Biol. Chem. **274:** 19874–19884.

Langbein, L., M. A. Rogers, H. Winter, S. Praetzel and J. Schweizer, 2001 The catalog of human hair keratins. II. Expression of the six type II members in the hair follicle and the combined catalog of human type I and II keratins. J. Biol. Chem. **27:** 35123–35132.

Langbein, L., M. A. Rogers, S. Praetzel, N. Aoki, H. Winter *et al.*, 2002 Novel epithelial keratin, hK6irs1, is expressed differentially in all layers of the inner root sheath, including specialized Huxley cells (Flugelzellen) of the human hair follicle. J. Invest. Dermatol. **118:** 789–799.

Lersch, R., and E. Fuchs, 1988 Sequence and expression of a type II keratin, K5, in human epidermal cells. Mol. Cell. Biol. **8:** 486–493.

Leube, R. E., F. X. Bosch, V. Romano, R. Zimbelmann, H. Hofler *et al.*, 1986 Cytokeratin expression in simple epithelia. III. Detection of mRNAs encoding human cytokeratins nos. 8 and 18 in normal and tumor cells by hybridization with cDNA sequences in vitro and in situ. Differentiation **33:** 69–85.

Leube, R. E., B. L. Bader, F. X. Bosch, R. Zimbelmann, T. Achtstaetter *et al.*, 1988 Molecular characterization and expression of the stratification-related cytokeratins 4 and 15. J. Cell Biol. **106:** 1249–1261.

Lynch, M. H., W. M. O'Guin, C. Hardy, L. Mak and T. T. Sun, 1986 Acidic and basic hair/nail ("hard") keratins: their colocalization in upper cortical and cuticle cells of the human hair follicle and their relationship to "soft" keratins. J. Cell Biol. **103:** 2593–2606.

Magin, T. M., 1998 Lessons from keratin transgenic and knockout mice. Subcell. Biochem. **31:** 141–172.

Manly, K. F., R. H. Cudmore, Jr. and J. M. Meer, 2001 Map Manager QTX, cross-platform software for genetic mapping. Mamm. Genome **12:** 930–932.

Miller, S. E., 2002 Molecular mechanisms regulating hair follicle development. J. Invest. Dermatol. 216–225.

Moll, R., W. W. Franke, D. L. Schiller, B. Geiger and R. Krepler, 1982 The catalog of human cytokeratins: patterns of expression in normal epithelia, tumors and cultured cells. Cell **31:** 11–24.

Moriwaki, K., 1994 Wild mouse from geneticist's viewpoint, pp. 13–14 in *Genetics in Wild Mice; Its Application to Biomedical Research*, edited by K. Moriwaki, T. Shiroishi and H. A. Yonekawa. Scientific Press/Karger, Tokyo.

O'Guin, W. M., A. Schermer, A. Lynch and T. T. Sun, 1990 Differentiation-specific expression of keratin pairs, pp. 301–334 in *Cellular and Molecular Biology of Intermediate Filaments*, edited by R. D. Goldman and P. M. Steinert. Plenum, New York.

Poirier, C., A. Yoshiki, K. Fujiwara, J. L. Guénet and M. Kusakabe, 2002 Hague (*Hag*): a new mouse hair mutation with an unstable semidominant allele. Genetics **162:** 831–840.

Porter, R. M., L. D. Corden, D. P. Lunny, F. J. Smith, E. B. Lane *et al.*, 2001 Keratin K6irs is specific to the inner root sheath of hair follicles in mice and humans. Br. J. Dermatol. **145:** 558–568.

Powell, B. C., and G. E. Rogers, 1990 Cyclic hair-loss and regrowth in transgenic mice overexpressing an intermediate filament gene. EMBO J. **9:** 1485–1493.

Rogers, M. A., H. Winter, C. Wolf, M. Heck and J. Schweizer, 1998 Characterization of a 190-kilobase pair domain of human type I hair keratin genes. J. Biol. Chem. **273:** 26683–26691.

Rogers, M. A., H. Winter, L. Langbein, C. Wolf and J. Schweizer, 2000 Characterization of a 300 kbp region of human DNA containing the type II hair keratin gene domain. J. Invest. Dermatol. **114:** 464–472.

Sambrook, J., E. F. Fritsch and T. Maniatis, 1989 *Molecular Cloning: A Laboratory Manual.* Cold Spring Harbor Laboratory Press, Cold Spring Harbor, NY.

Sato, H., T. Koide, H. Masuya, S. Wakana, T. Sagai *et al.*, 1998 A new mutation *Rim3* resembling *Re^{den}* is mapped close to retinoic acid receptor alpha (*Rara*) gene on mouse chromosome 11. Mamm. Genome **9:** 20–25.

Stark, H. J., D. Breitkreutz, A. Limat, C. M. Ryle, D. Roop *et al.*, 1990 Keratins 1 and 10 or homologues as regular constituents of inner root sheath and cuticle cells in the human hair follicle. Eur. J. Cell Biol. **52:** 359–372.

Steinert, P. M., D. A. Parry, W. W. Idler, L. D. Johnson, A. C. Steven *et al.*, 1985 Amino acid sequences of mouse and human epidermal type II keratins of Mr 67,000 provide a systematic basis for the structural and functional diversity of the end domains of keratin intermediate filament subunits. J. Biol. Chem. **260:** 7142–7149.

Takahashi, K., R. D. Paladini and P. A. Coulombe, 1995 Cloning and characterization of multiple human genes and cDNAs encoding highly related type II keratin 6 isoforms. J. Biol. Chem. **270:** 18581–18592.

Takahashi, K., B. Yan, K. Yamanishi, S. Imamura and P. A. Coulombe, 1998 The two functional keratin 6 genes of mouse are differentially regulated and evolved independently from their human orthologs. Genomics **53:** 170–183.

Taylor, L. A., M. J. Harris and D. M. Juriloff, 2000 Whiskers amiss, a new vibrissae and hair mutation near the *Krt1* cluster on mouse chromosome 11. Mamm. Genome **11:** 255–259.

Vassar, R., P. A. Coulombe, L. Degenstein, K. Albers and E. Fuchs, 1991 Mutant keratin expression in transgenic mice causes marked abnormalities resembling a human genetic skin disease. Cell **64:** 365–380.

Vasseur, M., P. Duprey, P. Brulet and F. Jacob, 1985 One gene and one pseudogene for the cytokeratin endo A. Proc. Natl. Acad. Sci. USA **82:** 1155–1159.

Winter, H., L. Langbein, S. Praetzel, M. Jacobs, M. A. Rogers *et al.*, 1998 A novel human type II cytokeratin, K6hf, specifically expressed in the companion layer of the hair follicle. J. Invest. Dermatol. **111:** 955–962.

Wojcik, S. M., S. Imakado, T. Seki, M. A. Longley, L. Petherbridge *et al.*, 1999 Expression of MK6a dominant-negative and C-terminal mutant transgenes in mice has distinct phenotypic consequences in the epidermis and hair follicle. Differentiation **65:** 97–112.

Communicating editor: N. Takahata